Observation of an extremely-long-lived metastable level in a Ti-like system via an *L*-shell dielectronic recombination measurement in highly charged 3*dⁿ* ions of tungsten

B. Tu,[1] K. Yao,[1] Y. Shen,[1] Y. Yang,[1] M. C. Li,[1] T. H. Xu,[1] Q. F. Lu,[1] D. Lu,[1] X. Wang,[1] C. Y. Chen,[1] Y. Fu,[1] B. Wei,[1]
C. Zheng,[1] L. Y. Huang,[1] G. Xiong,[1,2] J. M. Yang,[2] B. H. Zhang,[2] Y. J. Tang,[2] R. Hutton,[1] Y. Zou,[1,*] and J. Xiao[1,†]

[1]*Shanghai EBIT Laboratory, Institute of Modern Physics, and Key Laboratory of Nuclear Physics and Ion-beam Application (MOE),
Fudan University, Shanghai 200433, China*
[2]*Research Center of Laser Fusion, China Academy of Engineering Physics, P.O. Box 919-986, Mianyang 621900, China*

In this paper we report the *L*-shell dielectronic recombination measurement in highly charged 3*dⁿ* ions of tungsten by employing a fast electron beam-energy scanning technique at Shanghai EBIT. The studies of the *LMM* DR resonance strengths of Ar-like up to Mn-like tungsten were implemented through the experiment as well as a fully relativistic configuration interaction method in the flexible atomic code. In the analysis of DR spectrum, an isolated resonant peak was discovered coming from the DR processes via an extremely-long-lived metastable level in a Ti-like system. This work indicated the population of this Ti-like metastable level in the present EBIT plasma condition was as large as 45%.

I. INTRODUCTION

The metastable levels of atoms and ions, which decay to the ground or the lower levels via forbidden transitions such as magnetic dipole (M1), electric quadrupole (E2), or higher order magnetic or electric multipole transitions, are generally able to live very long with the lifetimes of the order of seconds or more. The radiation from these metastable levels are crucial for proper application of density diagnostics used in astrophysical and laboratory plasmas due to their sensitivity to the collisional effects in different plasma density conditions [1,2]. Some unusual atomic system with long-lived metastable levels creating an unperturbed well-defined ideal two-level system could have the potential applications in quantum information, atomic clocks, and searching for the variation of fundamental constants [3,4]. Furthermore, the long-lived metastable levels with high order forbidden transitions are desirable candidates for the study of hyperfine induced transitions [5,6] and magnetic induced transitions [7] since the lifetimes of these levels can be significantly affected through the new decay channels. Up to now, one metastable level with an ultralong lifetime of 10 years in ^{172}Yb$^+$ was determined experimentally by using quantum jumps in an electrodynamic trap [4] and another metastable level in Sn-like Pr^{9+} was predicted with a lifetime of 21 000 000 years in theory [3]. This sort of extremely-long-lived level can be counted as a second ground state, in the consequence owning the ground state properties, producing some new processes of collisional excitation and de-excitation, collisional ionization, and recombination through this metastable level, which is of importance in hot plasma models [8].

Dielectronic recombination (DR) is one of the electron ion recombination processes and used to be considered as a resonant two-step process. In the first step, as a free electron is captured by an ion, a bound electron of the ion is promoted, forming an intermediate multiply excited level sitting above

the ionization threshold. In the second step called radiative stabilization, photons are emitted to reduce the energy of the intermediate level to where it is below the ionization threshold. The other electron ion recombination process named as radiative recombination (RR) is that a free electron is captured by an ion following by one photon emission directly. DR plays an important role in the high temperature plasma [9–11]. It affects the charge state distribution and the ion level population, degrades the plasma temperature, and produces lots of satellite lines which are very useful in plasma diagnostics. Much work has been done to study the DR process in experiment at a heavy ion storage ring and electron beam ion trap (EBIT) [12–15]. Most of them reported the DR resonances measurements are from the ground states, while only a small part of work has observed the resonances of metastable levels at storage rings [16–20]. In an EBIT, the observation of DR processes from the metastable level is rare in experiment, only in the measurements of He- to O-like Si ions at HYPER-EBIT, Baumann *et al.* indicated the significant discrepancy between the experiment and the theory is caused by the influence of metastable levels [21], while further identifications of the metastable levels' resonances cannot be accomplished from the spectrum.

In this work, an extremely-long-lived metastable level in highly charge Ti-like tungsten ions is reported via the *L*-shell DR experiment at Shanghai EBIT [22]. A distinct resonance peak from a Ti-like long-lived metastable level was recognized in the DR spectrum. Furthermore, the *LMM* DR resonance strengths of Ar- up to Mn-like tungsten ions were determined in both experiment and theory.

II. EXPERIMENT

The experimental setup of *L*-shell DR measurement is similar with our previous work [23]. During the experiment, W(CO)$_6$ was continuously injected into the EBIT, and highly charged tungsten ions were produced by the collision with the electron beam. The beam energy was adjusted by employing an energy-fast-scanned technique. It was first set at 7.84 keV for charge breeding, then linearly scanned down to 3.26 keV in

*zouym@fudan.edu.cn
†xiao_jun@fudan.edu.cn

TABLE I. Experimental operating parameters at Shanghai EBIT.

Parameter	Value
Electron energy scanned	$7.84 \sim 3.26$ keV
Charge breeding energy	7.84 keV
Electron beam current	20 mA
Gas injection pressure	1.7×10^{-7} Torr
Trapping potential	80 V
Electron energy spread	43 eV

12 ms covering the resonance region of *L*-shell DR processes, and scanned back with the same rate. Before the next scanning cycle started, the beam energy was tuned at 7.84 keV for another 24 ms to maintain the charge state balance. The experimental operating parameters are listed in Table I.

The x-ray photons emitted from the highly charged tungsten ions were recorded by the high purity germanium detector that was fixed perpendicular to the electron beam. An event-mode data acquisition system was triggered by an arrival of the x ray, so that the photon energy together with the corresponding electron energy could be recorded simultaneously forming a scatter plot as shown in Fig. 1. In this figure, the resonance peaks are from *L*-shell DR processes labeled as *LMM*, *LMN*, *LMO*, *LMP*, ... sequence. The clear diagonal bands represent the RR processes with a free electron falling into the inner shells with quantum number of $n = 3$, $n = 4$, and higher. The raw data of *LMM* DR peaks and $n = 3$ RR process were then cut and projected onto the electron energy axis to obtain the excitation function, as shown in Fig. 2.

III. DATA ANALYSIS

The isolated DR resonance strength from an initial level *i* via an intermediate level *d* to a final level *f* can be expressed by [23]

$$S_{idf} = \int_{-\infty}^{+\infty} \sigma_{idf}(E)dE = \frac{g_d}{2g_i} \frac{\pi^2 \hbar^3}{m_e E_{res}} \frac{A_r(d \to f)A_a(d \to i)}{\sum A_r + \sum A_a},$$
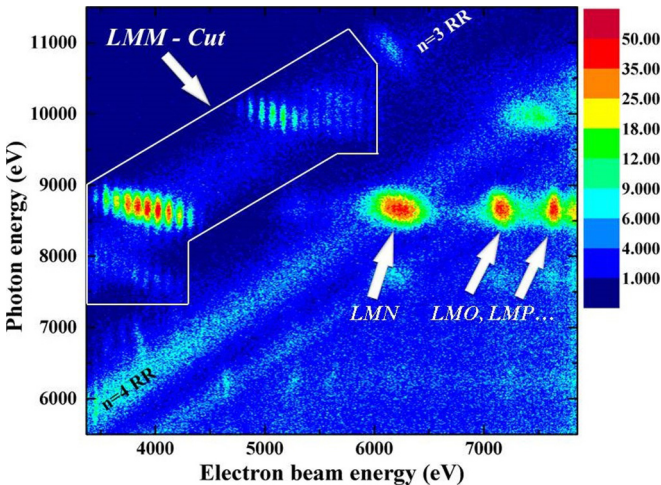(1)

FIG. 1. 2D scatter plot of x-ray intensity as a function of electron beam energy (*x* axis) and photon energy (*y* axis).
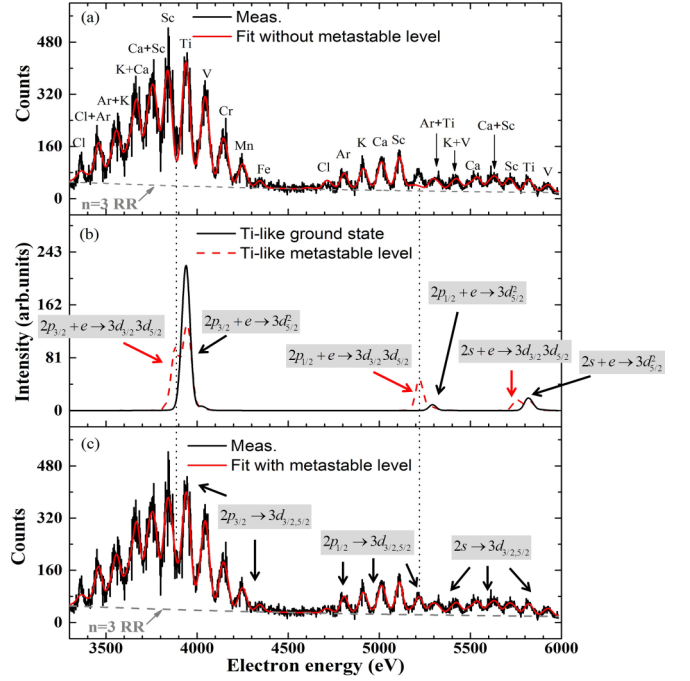

FIG. 2. The recombination excitation function of Cl- up to Fe-like *LMM* DR resonances. (a) The experimental curve (black) and fitted curve (red) without metastable level contribution. (b) The DR resonances through the ground (black solid) and metastable level (red dash) of Ti-like. (c) The experimental curve (black) and fitted curve (red) with Ti-like metastable level contribution. The gray dashed lines show the contribution of $n = 3$ RR.

where $\sigma_{idf}(E)$ is the DR cross section and g_d and g_i are the statistic weights of the levels *d* and *i*, respectively. E_{res} denotes the resonant energy. A_r is the spontaneous emission rate coefficient, and A_a is the autoionization rate.

The recombination excitation function for DR and RR processes can then be expressed by

$$C(q,E) = D(E)f_q \left[\frac{d\sigma_{RR}(q,E)}{d\Omega} + K_q \frac{\sum_{idf} S_{idf} W_{idf}(90°)}{4\pi} DR(E) \right],$$
(2)

where f_q denotes the ion abundance for the charge state *q*. $d\sigma_{RR}(q,E)/d\Omega$ is the differential cross section of $n = 3$ RR and $W_{idf}(90°)$ is the polarization and angular distribution coefficient for the electric dipole transition at $90°$ to the electron beam. $D(E)$ is the detection coefficient including the electron and ion density, overlap factor, detector efficiency (quantum efficiency and detection solid angle), detection time, etc. Since only the relative cross section of *LMM* DR to $n = 3$ RR process was measured in this experiment by normalizing the DR spectra on the theoretical RR cross section, the detection coefficient $D(E)$ was treated as a free parameter in the fitting formula. S_{idf} is the DR resonance strength and K_q is the independent amplitude factor used for correcting theoretical resonance strengths. $DR(E)$ represents the energy distribution of the resonance profile. In this excitation function, $S_{idf}(E)$ and f_q are the free parameters. While the resonance

TABLE II. Fitted charge state distribution f_q in the present experiment.

Cl	Al	K	Ca	Sc	Ti	V	Cr	Mn	Fe	Co
<1%	1%	2.9%	6.8%	10.8%	15.4%	17.5%	14.8%	13.5%	10.5%	6.3%

energy E_{res} and angular distribution coefficient $W_{idf}(90°)$ are calculated using the relativistic configuration interaction (RCI) method by employing flexible atomic code (FAC) [24]. The differential cross sections of $n = 3$ RR for incident electrons in the energy region of 3.3–6 keV are also calculated by FAC. The experimental *LMM* DR spectrum of W ions was then fitted via a least-squares method with the theoretical S_{idf} as the initial value. The fitting results of charge state distribution are listed in Table II.

In the RCI calculation for *LMM* DR processes, the configuration interactions in the calculation of wave function for the initial level included all the configurations of $[core][3s3p]^m 3d^{(u+8-m)}$ and $[core][3s3p]^m 3d^{(u+7-m)}nl$; in the same treatment, all the possible configurations of $1s^2[2s2p]^7[3s3p]^m 3d^{(u+10-m)}$, $1s^2[2s2p]^7[3s3p]^{m'} 3d^{(u+9-m')}4l$, and $[core][3s3p]^{m'} 3d^{(u+9-m')}$ were included for the intermediate level; the configurations of $[core][3s3p]^m 3d^{(u+9-m)}$ and $[core][3s3p]^m 3d^{(u+8-m)}nl$ for the final level. Here $m = 6, 7, 8$, $m' = 7, 8$, $n = 4, 5$, and [core] represents the closed shell $[1s^2 2s^2 2p^6]$. l included all the possible angular momentum and u from 1 to 6 represent K- up to Cr-like ions. For Ar-like ions, the configuration interactions for the initial level included $[core][3s3p]^8$, $[core][3s3p]^k 3d^{(8-k)}$, and $core[3s3p]^k 3d^{(7-k)}nl$ with $k = 6, 7$ and $n = 4, 5$; for Mn-like ions, the configuration interactions for the intermediate level included $1s^2[2s2p]^7[3s3p]^{k'} 3d^{(17-k')}$, $1s^2[2s2p]^7[3s3p]^{k'} 3d^{(16-k')}4l$, and $[core][3s3p]^{k'} 3d^{(16-k')}$ with $k' = 7, 8$. The treatments for the configuration interactions of other levels in Ar- and Mn-like ions are the same as K- up to Cr-like ions. For the electron-electron interaction, both Coulomb and Breit effects were taken into account.

IV. RESULT AND DISCUSSION

The *LMM* DR spectra of Cl- up to Fe-like W ions were shown in Fig. 2, in which the resonance peaks are distinct in two separate energy regions of 3.3–4.4 keV and 4.6–6.0 keV. In the lower energy region, the DR resonances involve the inner *L*-shell $2p_{3/2}$ excitation to *M*-shell $3d_{3/2}$ or $3d_{5/2}$, while those resonance peaks lying in the higher energy region involve the $2p_{1/2}$ or $2s$ excitation to $3d_{3/2}$ or $3d_{5/2}$ orbits. In Fig. 2(a) the fitted curve (red) based on our RCI calculations shows good agreement with the experimental curve (black) and those DR peaks marked out in the spectrum match our synthetic spectrum very well except for one isolated resonance peak in the energy region of 5180–5250 eV. The electron beam energy was precisely calibrated by a high voltage divider [25] in the experiment, and the space charge effect is about 50 eV at 3.3 keV. As a result, the misidentification of the DR resonances cannot happen and the new isolated peak definitely reveals the new DR resonances which are not taken into account in this synthetic spectrum.

According to our energy level calculation on Ti-like W ions, a very long-lived metastable level was discovered in the present work. Figure 3 shows the theoretical energy levels for the ground configuration $[core]'(3d_{3/2}^4)$ ([core]' represents $1s^2 2s^2 2p^6 3s^2 3p^6$) and the first excited configuration $[core]'(3d_{3/2}^3 3d_{5/2})$ of Ti-like ions. This RCI calculation has been compared with other theoretical results in the earlier studies [26,27] and the agreement within 0.1%–0.4% in the energy levels calculation of the first excited configuration of Ti-like W ions was achieved. The theoretical result demonstrates the metastable level of $[core]'(3d_{3/2}^3 3d_{5/2})_4$ can only decay through an electric 16 pole or a magnetic octupole forbidden transition to the lower levels of $[core]'(3d_{3/2}^4)_0$ or $[core]'(3d_{3/2}^3 3d_{5/2})_1$, and the transition rates are 2.36×10^{-10} and 8.24×10^{-14} s^{-1}, respectively, which gives rise to the metastable level having a very long lifetime of about 143 years. This metastable level with such a long lifetime probably has a large amount of population in an EBIT plasma condition, and consequently the DR processes via this initial level should contribute to the DR spectrum. The comparison of the DR synthetic spectrum of Ti-like W ions through the inner shell excitation from the ground and this metastable level are shown in Fig. 2(b). The resonances coming from the ground show the isolated monopeaks for $2p_{3/2}$, $2p_{1/2}$, and $2s$ electron excitation in three distinct energy regions, while those resonances from the metastable level through the same inner shell excitation reveal the doublet-peak profile. The reason is that for the metastable level $[core]'(3d_{3/2}^3 3d_{5/2})_4$ an extra dielectronic capture (DC) process (the first step of DR) in which the promoted electron and free electron together form intermediate $3d_{3/2} 3d_{5/2}$ configuration is opened, while for the ground $core'(3d_{3/2}^4)_0$ with a full-populated $3d_{3/2}$ orbit the promoted electron and free electron can only form $3d_{5/2}^2$
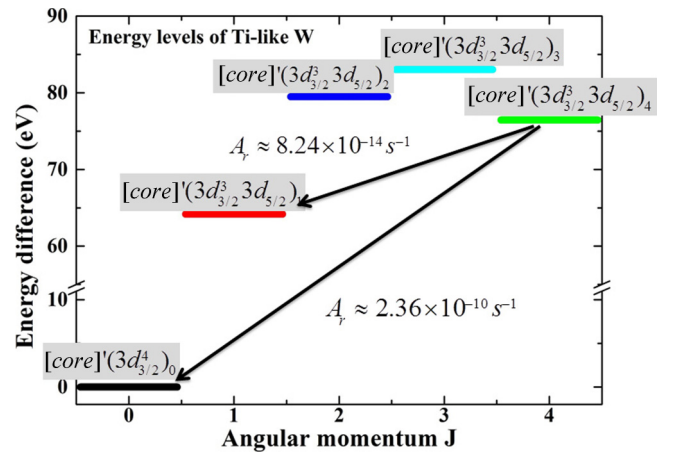

FIG. 3. Levels diagram for the ground $[core]'(3d_{3/2}^4)$ and first excited configuration $[core]'(3d_{3/2}^3 3d_{5/2})$ of Ti-like W ions.

configuration. In the previous DC process forming $3d_{3/2}3d_{5/2}$ configuration, the resonant energy is lower than that in the latter process forming $3d_{5/2}^2$ configuration by the energy difference between $3d_{3/2}$ and $3d_{5/2}$ orbit with the same inner shell electron excitation. Furthermore, this resonant energy difference of these two DC processes via the metastable level can be distinguished based on the present electron energy resolution so as to show the doublet-peak profile in the DR spectrum. The resonant peak for the metastable level involving the inner shell $2p_{1/2}$ electron excitation forming $3d_{3/2}3d_{5/2}$ configuration matches that unidentified peak in Fig. 2(a) very well in both electron energy axis and the relative intensity of resonances.

A refined least-square fitting for the experimental spectrum, which included the DR resonances through the Ti-like metastable level $[\text{core}]'(3d_{3/2}^3 3d_{5/2})_4$, was implemented to show very good agreement with our measurement in Fig. 2(c). The unidentified peak at around 5180–5250 eV in Fig. 2(a) was well fitted by including the metastable level's DR resonances. In addition, the deficit at around 3885 eV, although it is not remarkable in the fitted excitation function comparing with the experimental spectrum in Fig. 2(a), was also filled by the Ti-like metastable level's resonances involving the inner shell $2p_{3/2}$ electron excitation as shown in Figs. 2(b) and 2(c). Based on our calculation, the $n = 3$ RR cross section of the metastable level is very close to that of the ground so that the population of the metastable level is not able to affect the total RR strength.

The fitted resonance strengths together with the corresponding theoretical ones of Al- up to Mn-like *LMM* DR W ions are listed in Table III. The total uncertainties of the experimental resonances strengths are less than 15%, except for Mn-like ions of 22% due to the less statistics of the Mn-like resonance peaks. The first uncertainty resource from the statistics and peaks mixing gave rise to the uncertainties of 5%–11% for most DR peaks and 18% for Mn-like peaks. The second contribution is from the RCI calculation of RR cross

TABLE III. The measured total resonance strengths $\sum S_{idf}^{\text{meas.}}$ (10^{-20} cm^2 eV) for Ar-like up to Mn-like *LMM* DR W ions, together with the theoretical results $\sum S_{idf}^{\text{calc.}}$ and the calculated mean angular distribution coefficient $\frac{\sum W_{idf} S_{idf}^{\text{calc.}}}{\sum S_{idf}^{\text{calc.}}}$.

Ion	Initial level	$\sum S_{idf}^{\text{calc.}}$	$\sum S_{idf}^{\text{meas.}}$	$\frac{\sum W_{idf} S_{idf}^{\text{calc.}}}{\sum S_{idf}^{\text{calc.}}}$
Ar	$[\text{core}]'$[a]	391	401(60)	1.13
K	$[\text{core}]'(3d_{3/2}^1)_{3/2}$	274	282(40)	1.02
Ca	$[\text{core}]'(3d_{3/2}^2)_2$	189	189(25)	0.99
Sc	$[\text{core}]'(3d_{3/2}^3)_{3/2}$	125	129(15)	1.04
Ti	$[\text{core}]'(3d_{3/2}^4)_0$	68.1	38.1(3.1) + 41.5(5.0)[b]	1.05
Ti*	$[\text{core}]'(3d_{3/2}^3 3d_{5/2})_4$	90.3		0.97
V	$[\text{core}]'(3d_{3/2}^4 3d_{5/2})_{5/2}$	40.5	40.6(3.9)	0.99
Cr	$[\text{core}]'(3d_{3/2}^4 3d_{5/2}^2)_4$	24.0	23.1(3.0)	1.00
Mn	$[\text{core}]'(3d_{3/2}^4 3d_{5/2}^3)_{9/2}$	11.3	11.2(2.5)	1.01

[a]$[\text{core}]'$ represents $1s^2 2s^2 2p^6 3s^2 3p^6$.
[b]Represents the calculated and measured DR strength from the Ti-like metastable level.

section, which is considered to give the accuracy within an error of about 3% (see [28] and references therein). The third is caused by the charge state variation in a single scanning cycle of electron beam energy during the experiment, which is estimated to be less than 1.2% by following [23,28]. The last source is from the cutoff of the resonances region at 6 keV. For V-, Cr-, and Mn-like W ions, a few resonances should be expected at the resonant energy higher than 6 keV according to our calculations; however, those peaks were too weak to be discovered in the 2D scatter plot and excluded in the fitting excitation function. In a consequence, the resonance peaks cutoff caused the errors of about 0.5%, 4.6%, and 3.5% based on the resonance strengths calculations for V-, Cr-, and Mn-like W ions, respectively. For Cl- and Fe-like ions, the statistics are not good enough to obtain the reliable fitting results, and thus the resonance strengths of those two charge states W ions were not given in this work.

The measured resonances strengths of Ar- up to Mn-like *LMM* DR W ions agree very well with our calculations within the experimental uncertainties. For Ti-like ion, the theoretical resonances strengths are 68.1 and 90.3 (10^{-20} eV) for the DR processes from the ground and long-lived metastable level, respectively, while the measured resonances strength is 79.6(8.1) the sum of 38.1(3.1) and 41.5(5.0) which are the experimental results of DR resonances strengths from Ti-like ground and metastable level, respectively. The discrepancy between the measurement and the calculations is because both the ground and long-lived metastable level which share the populations as the initial level contribute to the DR spectrum, and the relative population ratios can be derived from the measurement and calculation as $(55 \pm 8)\%$ and $(45 \pm 7)\%$ for the ground and metastable level, respectively.

In our DR experiment, the initial level population was determined during the period of charge breeding. In this work, a collisional radiative (CR) model was employed to simulate the population of the ground ($[\text{core}]'3d_{3/2}^4$) and first excitation ($[\text{core}]'3d_{3/2}^3 3d_{5/2}$) configurations for Ti-like W ions by FAC, which is similar to the theoretical spectra calculations of tungsten by Clementson *et al.* [29]. The present CR model including the atomic processes of electron impact excitation and de-excitation together with the E1, M1, E2, M2 type radiative decay involving the configurations of $[\text{core}][3s3p]^u[3d]^{(12-u)}$ and $[\text{core}][3s3p]^{u'}[3d]^{(11-u')}nl$ ($[\text{core}]$ represents $1s^2 2s^2 2p^6$) with $u = 6,7,8$, $u' = 7,8$, and $n = 4,5,6$ is the principle number relative to the total number of the configurations considered in the CR model. The higher order forbidden transitions are too weak to affect the calculated results of level populations and line intensities, therefore those type of transitions are not taken into account. The electron impact energy and electron beam density in the simulation are 7.9 keV and 5×10^{11} cm^{-3}, respectively, which match the experimental parameters in EBIT.

Our result shows the ground $[\text{core}]'(3d_{3/2}^4)_0$ and the long-lived metastable level $[\text{core}]'(3d_{3/2}^3 3d_{5/2})_4$ for Ti-like W ions share the most populations ($>99\%$) under the present experimental plasma condition. As the considered configurations increased, more cascades were included in the CR model, and the population of the long-lived metastable level is convergent up to about 30%. This theoretical result shows an apparent
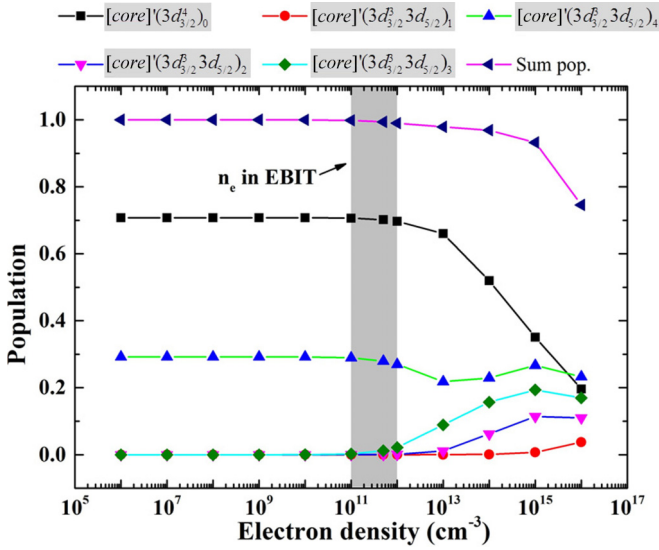
FIG. 4. The electron density dependence for the population of the ground and first excitation configurations of Ti-like W ions with the electron impact energy of 7.9 keV. The shadow shows the possible electron density of 10^{11}–10^{12} cm^{-3} in Shanghai EBIT.

discrepancy to the prediction of $(45 \pm 7)\%$ from our DR measurement, which is probably coming from the CR-model calculation. On one hand, the error of the atomic structure data used in the CR model, such as the collision strengths and transition rates, causes the uncertainty in the population calculation. On the other hand, the charge exchange process is not included in the present CR model in FAC, and in general higher charge W ions are certain to grab the electrons from the injected and background neutral atoms and subsequently leading to the changes of the population of Ti-like ions, although such charge exchange effect is usually not significant in the EBIT plasma environment.

The electron density dependence for the population of the ground and first excitation configurations of Ti-like W ions were also studied at the electron impact energy of 7.9 keV, as shown in Fig. 4. The result demonstrates the other short-lived

metastable levels with the calculated lifetime less than 1 ms occupy very few population in the EBIT electron density of 10^{11}–10^{12} cm^{-3}, therefore the DR processes from these levels cannot affect the determination of Ti-like long-lived metastable population in experiment. As the electron density increases, the population of the ground declines and those short-lived metastable levels start to share the populations, while the long-lived metastable level $[core]'(3d_{3/2}^3 3d_{5/2})_4$ shows very little dependence on the electron density. The stability characteristic for such a large-populated metastable level is of great importance in any plasma environment. Especially for fusion plasma, this extremely-long-lived metastable level of Ti-like W can be considered as a second ground, through which the processes of collisional excitation and de-excitation, collisional ionization and recombination give rise to some new transitions, resonances, and even indirect ionization processes affecting the charge state balance and radiation mechanism in hot plasma models.

V. CONCLUSIONS

In this article, an extremely-long-lived metastable level in Ti-like W ions was discovered via the dielectronic recombination experiment performed at Shanghai EBIT. In the comparison between the measured and the theoretical predicted resonance strengths of Ti-like levels, a large population of about $(45 \pm 7)\%$ for this long-lived metastable level was obtained in the present EBIT plasma condition. The CR model also demonstrated nearly independent behavior of the electron density that endows this level the characteristic as a second ground. Furthermore, the resonance strengths of *LMM* DR of Ar- up to Mn-like tungsten were determined in our experiment and the results showed very good agreement with our calculations by FAC.

[1] B. J. Wargelin, P. Beiersdorfer, and S. M. Kahn, Phys. Rev. Lett. **71**, 2196 (1993).

[2] B. Proxauf, S. Oettl, and S. Kimeswenger, Astron. Astrophys. **561**, A10 (2013).

[3] M. S. Safronova, V. A. Dzuba, V. V. Flambaum, U. I. Safronova, S. G. Porsev, and M. G. Kozlov, Phys. Rev. Lett. **113**, 030801 (2014).

[4] M. Roberts, P. Taylor, G. P. Barwood, P. Gill, H. A. Klein, and W. R. C. Rowley, Phys. Rev. Lett. **78**, 1876 (1997).

[5] K. Yao, M. Andersson, T. Brage, R. Hutton, P. Jönsson, and Y. Zou, Phys. Rev. Lett. **97**, 183001 (2006).

[6] E. Träbert, P. Beiersdorfer, and G. V. Brown, Phys. Rev. Lett. **98**, 263001 (2007).

[7] W. Li, J. Grumer, Y. Yang, T. Brage, K. Yao, C. Chen, T. Watanabe, P. Jönsson, H. Lundstedt, and R. Hutton, Astrophys. J. **807**, 69 (2015).

[8] Y. Kobayashi, D. Kato, H. A. Sakaue, I. Murakami, and N. Nakamura, Phys. Rev. A **89**, 010501(R) (2014).

[9] S. P. Preval, N. R. Badnell, and M. G. O'Mullane, Phys. Rev. A **93**, 042703 (2016).

[10] N. R. Badnell, K. Spruck, C. Krantz, O. Novotný, A. Becker, D. Bernhardt, M. Grieser, M. Hahn, R. Repnow, D. W. Savin *et al.*, Phys. Rev. A **93**, 052703 (2016).

[11] P. Beiersdorfer, M. May, J. Scofield, and S. Hansen, High Energy Density Phys. **8**, 271 (2012).

[12] G. Kilgus, J. Berger, P. Blatt, M. Grieser, D. Habs, B. Hochadel, E. Jaeschke, D. Krämer, R. Neumann, G. Neureither *et al.*, Phys. Rev. Lett. **64**, 737 (1990).

[13] D. W. Savin, T. Bartsch, M. H. Chen, S. M. Kahn, D. A. Liedahl, J. Linkemann, A. Müller, S. Schippers, M. Schmitt, D. Schwalm *et al.*, Astrophys. J. Lett. **489**, L115 (1997).

[14] D. A. Knapp, R. E. Marrs, M. B. Schneider, M. H. Chen, M. A. Levine, and P. Lee, Phys. Rev. A **47**, 2039 (1993).

[15] G. Xiong, J. Zhang, Z. Hu, N. Nakamura, Y. Li, X. Han, J. Yang, and B. Zhang, Phys. Rev. A **88**, 042704 (2013).

[16] L. H. Andersen, P. Hvelplund, H. Knudsen, and P. Kvistgaard, Phys. Rev. Lett. **62**, 2656 (1989).

[17] L. H. Andersen, G.-Y. Pan, H. T. Schmidt, N. R. Badnell, and M. S. Pindzola, Phys. Rev. A **45**, 7868 (1992).

[18] A. A. Saghiri, J. Linkemann, M. Schmitt, D. Schwalm, A. Wolf, T. Bartsch, A. Hoffknecht, A. Müller, W. G. Graham, A. D. Price *et al.*, Phys. Rev. A **60**, R3350 (1999).

[19] S. Schippers, G. Gwinner, C. Brandau, S. Böhm, M. Grieser, S. Kieslich, H. Knopp, A. Müller, R. Repnow, and D. Schwalm, Nucl. Instrum. Methods Phys. Res. B **235**, 265 (2005).

[20] D. Bernhardt, C. Brandau, Z. Harman, C. Kozhuharov, S. Böhm, F. Bosch, S. Fritzsche, J. Jacobi, S. Kieslich, and H. Knopp, J. Phys. B **48**, 144008 (2015).

[21] T. M. Baumann, Z. Harman, J. Stark, C. Beilmann, G. Liang, P. H. Mokler, J. Ullrich, and J. R. Crespo López-Urrutia, Phys. Rev. A **90**, 052704 (2014).

[22] D. Lu, Y. Yang, J. Xiao, Y. Shen, Y. Fu, B. Wei, K. Yao, R. Hutton, and Y. Zou, Rev. Sci. Instrum. **85**, 093301 (2014).

[23] B. Tu, J. Xiao, Y. Shen, Y. Yang, D. Lu, T. H. Xu, W. X. Li, C. Y. Chen, Y. Fu, B. Wei *et al.*, Phys. Plasmas **23**, 053301 (2016).

[24] M. F. Gu, Can. J. Phys. **86**, 675 (2008).

[25] W. D. Chen, J. Xiao, Y. Shen, Y. Q. Fu, F. C. Meng, C. Y. Chen, B. H. Zhang, Y. J. Tang, R. Hutton, and Y. Zou, Phys. Plasmas **15**, 083301 (2008).

[26] X. L. Guo, M. Huang, J. Yan, S. Li, R. Si, C. Y. Li, C. Y. Chen, Y. S. Wang, and Y. M. Zou, J. Phys. B **48**, 144020 (2015).

[27] P. Quinet, J. Phys. B **44**, 195007 (2011).

[28] K. Yao, Z. Geng, J. Xiao, Y. Yang, C. Chen, Y. Fu, D. Lu, R. Hutton, and Y. Zou, Phys. Rev. A **81**, 022714 (2010).

[29] J. Clementson, P. Beiersdorfer, T. Brage, and M. Gu, At. Data Nucl. Data Tables **100**, 577 (2014).